1-Alpha, 25-dihydroxyvitamin D3 alters the pharmacokinetics of mycophenolic acid in renal transplant recipients by regulating two extrahepatic UDP-glucuronosyltransferases 1A8 and 1A10

XIAOLIANG WANG[1], HONGWEI WANG[1], BING SHEN, BRIAN R. OVERHOLSER, BRUCE R. COOPER, YINGHAO LU, HUAMEI TANG, CHONGZHI ZHOU, XING SUN, LIN ZHONG, MURRAY J. FAVUS, BRIAN S. DECKER, WANQING LIU[2], and ZHIHAI PENG[2]

SHANGHAI AND GUIYANG, P. R. CHINA; WEST LAFAYETTE, IND AND CHICAGO, ILL, USA

Mycophenolic acid (MPA) is an important immunosuppressant broadly used in renal transplantation. However, the large inter-patient variability in mycophenolic acid (MPA) pharmacokinetics (PK) limits its use. We hypothesize that extrahepatic metabolism of MPA may have significant impact on MPA PK variability. Two intestinal UDP-glucuronosyltransferases 1A8 and 1A10 plays critical role in MPA metabolism. Both *in silico* and previous genome-wide analyses suggested that vitamin D (VD) may regulate intestinal *UGT1A* expression. We validated the VD response elements (VDREs) across the *UGT1A* locus with chromatin immunoprecipitation (ChIP) and luciferase reporter assays. The impact of 1-alpha,25-dihydroxyvitamin D3 (D3) on *UGT1A8* and *UGT1A10* transcription and on MPA glucuronidation was tested in human intestinal cell lines LS180, Caco-2 and HCT-116. The correlation between transcription levels of VD receptor (VDR) and the two UGT genes were examined in human normal colorectal tissue samples (n = 73). PK alterations of MPA following the parent drug, mycophenolate mofetil (MMF), and D3 treatment was assessed among renal transplant recipients (n = 10). Our ChIP assay validate three VDREs which were further demonstrated as transcriptional enhancers with the luciferase assays. D3 treatment significantly increased transcription of both UGT genes as well as MPA glucuronidation in cells. The *VDR* mRNA level was highly correlated with that of both *UGT1A8* and *UGT1A10* in human colorectal tissue. D3 treatment in patients led to

[1] Both authors contributed equally to this work.
[2] Joint senior authors.

From the Department of General Surgery, Shanghai First People's Hospital, Medical College, Shanghai Jiaotong University, Shanghai, P. R. China; Department of Medicinal Chemistry & Molecular Pharmacology, College of Pharmacy, Purdue University, West Lafayette, Ind, USA; Section of Endocrinology, Department of Medicine, The University of Chicago, Chicago, Ill, USA; Department of Urology, Shanghai First People's Hospital, Medical College, Shanghai Jiaotong University, Shanghai, P. R. China; Department of Pharmacy Practice, College of Pharmacy, Purdue University, West Lafayette, Ind, USA; Bindley Bioscience Center, Metabolite Profiling Facility, Purdue University, West Lafayette, Ind, USA; Department of Hematology, Affiliated Hospital of Guiyang Medical College, The Hematopoietic Stem Cell Transplant Center of Guizhou Province, Guiyang, P. R. China; Department of Pathology, Shanghai First People's Hospital, Medical College, Shanghai Jiaotong University, Shanghai, P. R. China; Division of Nephrology, School of Medicine, Indiana University, Indianapolis, Ind, USA; Department of Medicine, School of Medicine, Indiana University, Indianapolis, Ind, USA.

Submitted for publication October 15, 2015; revision submitted May 31, 2016; accepted for publication July 7, 2016.

Reprint requests: Wanqing Liu, Department of Medicinal Chemistry & Molecular Pharmacology, College of Pharmacy, Purdue University. 575 Stadium Mall Dr, West Lafayette, IN 47907, USA; e-mail: liu781@purdue.edu or Zhihai Peng, Department of General Surgery, Shanghai General Hospital, Shanghai Jiao Tong University School of Medicine. 100 Haining Road, Shanghai, 200080, The People's Republic of China; e-mail: pengzhihai@sjtu.edu.cn.

1931-5244

http://dx.doi.org/10.1016/j.trsl.2016.07.006

about 40% reduction in both AUC_{0-12} and Cmax while over 70% elevation of total clearance of MPA. Our study suggested a significant regulatory role of VD on MPA metabolism and PK via modulating extrahepatic UGT activity. (Translational Research 2016;178:54–62)

Abbreviations: AcMPAG = acyl mycophenolic acid glucuronide; ChIP = chromatin immunoprecipitation; Cmax = maximum concentration; DR = direct repeat; MMF = mycophenolate mofetil; MPA = mycophenolic acid; MPAG = mycophenolic acid glucuronide; PK = pharmacokinetics; PD = pharmacodynamics; TDM = therapeutic drug monitoring; UGT = UDP-glucuronosyltransferase; VDR = Vitamin D3 receptor; VDRE = Vitamin D response element

AT A GLANCE COMMENTARY

Wang X, et al.

Background

Mycophenolic acid (MPA) is an important immunosuppressant, but the large inter-patient variability in its pharmacokinetics (PK) limits its use. Our study found that 1-alpha,25-dihydroxyvitamin D3 (VD) regulates the transcription of two intestinal UDP-glucuronosyltransferases *UGT1A8* and *UGT1A10* which are involved in glucuronidation of MPA, which has a significant impact on MPA pharmacokinetics in kidney transplant recipients.

Translational Significance

Our study identified a novel mechanism underlying the inter-patient variability in MPA pharmacokinetics, and suggests co-administration of VD with MPA may potentially result in drug-drug interaction and lead to inter- and intra-patient difference in clinical response to MPA treatment.

INTRODUCTION

Mycophenolate mofetil (MMF) is increasingly used as an important immunosuppressant to prevent acute rejection after kidney transplantation. Recent clinical studies have consistently suggested that including MMF is superior to other immunosuppressant combinations in maintaining renal function, in the development of adverse effects, as well as in graft and patient survival.[1-4] However, inter-patient variability in its pharmacokinetics (PK) limits its full potential in clinical applications.[5,6] MMF is a prodrug which is hydrolyzed into its active form mycophenolic acid (MPA) after oral intake.[5] It has been shown that the extent of MPA exposure is highly correlated with acute allograft rejection.[7] About 20% of patients discontinue the medication due to the adverse events such as gastrointestinal disorders and bone marrow suppression which were suggested to be associated with the free MPA fraction.[7,8] In spite of numerous studies to date, the mechanism underlying this inter-patient PK variability of MMF/MPA has not been completely elucidated.[6] In order to individualize the MMF dosage, current MMF administration protocols increasingly apply therapeutic drug monitoring (TDM).[7,9] Therefore, identifying factors affecting MMF/MPA PK is of particular importance to achieve more effective and safer use of this drug.

Inter-patient PK variability are largely attributed to the variable activities of drug metabolism pathways. Previous studies have demonstrated that MPA is mainly metabolized via glucuronidation by UDP-glucuronosyltransferases (UGTs) in both the liver and intestine, which produces a major phenolic glucuronide, mycophenolic acid glucuronide (MPAG), and a minor acyl glucuronide (AcMPAG).[10-14] UGTs catalyze the formation of hydrophilic glucuronides, which is one of the important detoxification processes in human metabolism.[15] The human UGTs consists of 4 families, UGT1, UGT2A and 2B, UGT3, and UGT8, of which, UGT1, UGT2A and UGT2B are primarily involved in drug metabolism and are encoded by genes located on chromosome 2 and 4, respectively.[15-17] Variability in UGT activity has been significantly associated with inter-individual differences in metabolism of a broad array of endogenous and exogenous compounds including many therapeutic agents.[18] Previous studies have revealed that glucuronidation of MPA mainly involves UGT1A8 and UGT1A9, with UGT1A10 and UGT2B7 playing a minor role.[10-14] While UGT1A9 and UGT2B7 are important hepatic UGTs whose roles in MPA metabolism have been widely investigated, UGT1A8 and UGT1A10 are the only two UGT1A enzymes expressed in human intestinal tissue including the small intestine, colon and rectum,[15,19] and their roles in MPA PK variability has drawn only limited attention. It has been suggested that intestinal UGTs are also critical to the metabolism of many

compounds.[20,21] Therefore, variability in the activities of these two enzymes may also significantly contribute to the inter-patient difference in both the pharmacokinetics and pharmacodynamics of MMF/MPA.

On the other hand, as one of the most important transcription factors in human intestinal tissue, the vitamin D receptor (VDR) plays a crucial role in regulating a large number of genes.[22,23] A recent genome-wide study using a human intestinal cell line LS180 revealed that *UGT1A* locus harbors multiple vitamin D response elements (VDREs), and *UGT1A* gene expression is significantly induced by 1-alpha,25-dihydroxyvitamin D_3 [$1\alpha,25(OH)_2D_3$] treatment.[24] Given that only 1 cell line was tested in this study, additional VDREs may also exist e.g. in a cell-specific manner, we further performed an *in silico* screening for putative VDREs (the most common DR3-type)[25] in the *UGT1A8* and *UGT1A10* region as well as the entire *UGT1A* locus. We have identified a number of putative VDREs in this region. On the other hand, our previous study has suggested that VDR is not a significant regulator for hepatic UGTs, further underscores the importance of potential VDR-UGT regulation in intestinal tissues. We therefore hypothesize that VD/VDR is an important regulator for intestinal UGTs 1A8 and 1A10, which may further influence the MPA metabolism. In order to corroborate this hypothesis, we performed studies in human colorectal cancer cell lines and tissue samples aiming to: 1) validate the binding of VDR to the putative VDREs; 2) examine the effects of $1\alpha,25(OH)_2D_3$ treatment in regulating *UGT1A8* and *UGT1A10* mRNA expression and enzyme activity in MPA glucuronidation; and 3) examine the effects of $1\alpha,25(OH)_2D_3$ on MMF/MPA PK profiles in human kidney transplantation patients.

METHODS

Human tissue samples and kidney transplantation patients. Human colorectal (n = 73) mucosa tissue samples were collected at the time of surgery from pathologically documented colorectal cancer patients at the Shanghai First People's Hospital (Shanghai, China) with informed consent and conformation with institutional guidelines. All collected normal tissue were >5 cm away from the primary tumor site. The patients are all Han Chinese in origin with a median age of 68 years, and 50% of whom were female.

Kidney transplantation recipients (n = 10) were recruited to test the impact of vitamin D on the MPA PK profiles. Patient information was summarized in Table SII. All participants are inpatients of the Transplantation Center at the Shanghai First People's Hospital. Informed consent was obtained from all participants and was in conformation with institutional guidelines.

The collection of human tissue samples as well as the human subject study was approved by Institutional Review Board (IRB) of the Shanghai First People's Hospital.

In silico screening for putative VDREs. The most typical DR (direct repeat) 3-type VDRE was screened by a bioinformatic analysis (detailed in supplement methods) of the genomic sequence spanning the entire *UGT1A* gene locus as well as ±100kb flanking sequences (a total of 352,020 bp).

Chromatin immunoprecipitation (ChIP) assay. The ChIP assay (detailed in supplement methods) was performed in LS180, Caco-2 and HCT-116 cells under treatment with 10^{-8} M $1\alpha,25(OH)_2D_3$ or vehicle (ethanol) at 1, 8 and 24 hr time points, respectively.

Cloning and luciferase assay. The DNA fragments containing the putative VDREs were cloned into the pGL3-Promoter (pGL3-P) vector (Promega, WI, USA), and transiently transfected into the LS180 cells, respectively, using Lipofectamine® 2000 Transfection Reagent (Life Technologies, CA, USA) according to the manufacturer's instructions. After 24 hrs of transfection, luciferase activity was compared between the transfection of pGL3-Promoter (pGL3-P) and pGL3-Promoter-VDRE vectors with or without $1\alpha,25(OH)_2D_3$ treatment (10^{-8} M) by using the Dual-Luciferase® Reporter Assay System (Promega).

Real-time PCR. Transcription levels of *UGT1A8*, *UGT1A10* and/or *VDR* in the cell lines before and after $1\alpha,25(OH)_2D_3$ treatment (10^{-8} M for 24 hrs), as well as in human normal colorectal tissue samples (n = 73) were quantified with real-time PCR.

Effects of $1\alpha,25(OH)_2D_3$ treatment on MPA glucurondiation in cell lines. LS180, Caco-2 and HCT-116 cells were treated with $1\alpha,25(OH)_2D_3$ (10^{-8} M) or vehicle for 24 or 48 hrs, followed by co-incubation with MPA (2 mM) and UDPGA (0.5 mM) for additional 4 hrs. MPA glucuronidation rates were measured using HPLC/MS/MS. Briefly, the peak areas of MPA and MPAG were calculated and the ratio of MPAG/MPA were normalized to the mean values of the ratios of triplicates. These normalized ratios were then reported as the endpoint data. Assays were performed in triplicates and repeated twice. (See details in supplement methods).

Effect of $1\alpha,25(OH)_2D_3$ treatment on MPA PK profiles in vivo. We recruited kidney transplantation recipients (n = 10) who all underwent kidney transplantation 14–15 days prior to the PK study. Baseline Creatinine, Creatinine Clearance (CrCL) and albumin levels for all patients were collected (Table SII). Cyclosporine A (CsA) and prednisone were administrated for all

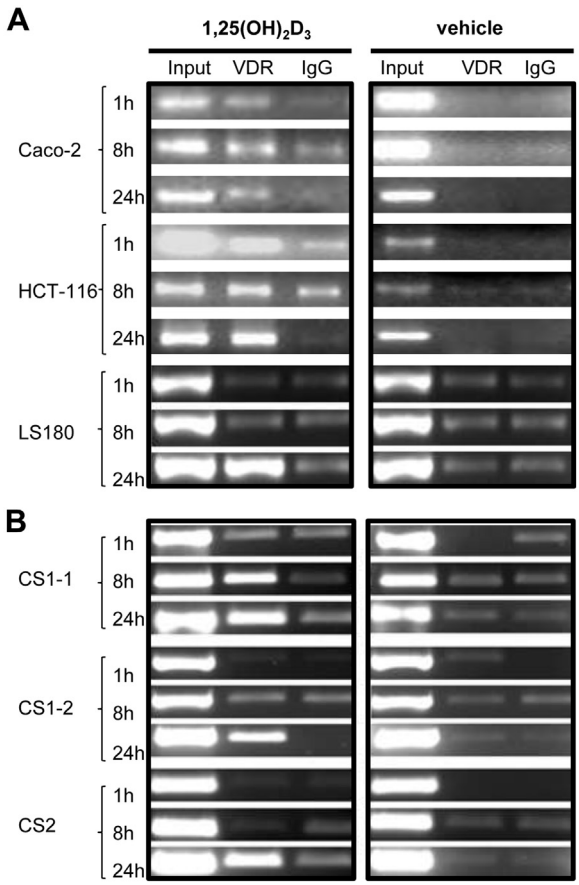

Fig 1. Chromatin Immunoprecipitation (ChIP) assays for validating the VDR binding to the *UGT1A* locus. **A**). ChIP assays for VDRE16 identified from the 5′-flanking sequence of *UGT1A8* exon 1 region among all 3 cell lines. **B**). ChIP assays for CS1 and CS2 identified in previous ChIP-seq study[24] in LS180. Note that two amplicons were examined in the CS1 region. Data were shown for the time points at 1, 8 and 24 hr of treatment with $1\alpha,25(OH)_2D_3$ or vehicle (ethanol) only. A significantly stronger band in the anti-VDR group as compared to the IgG group (negative control) indicates a positive VDR binding to the region.

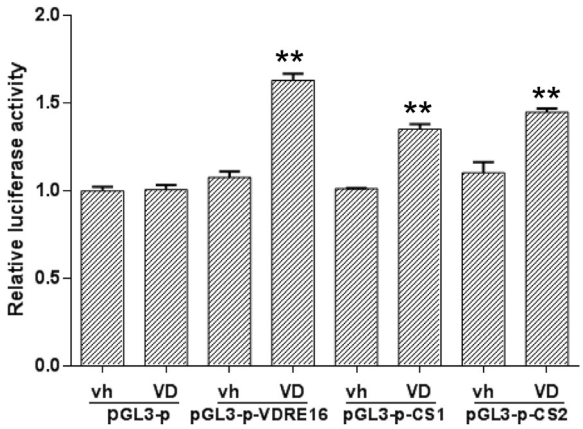

Fig 2. Regulatory function of the identified VDREs as transcriptional enhancers by luciferase assay. Data are shown as mean ± SD. $^{**}P < 0.01$. *P* values were calculated based on the comparison in relative luciferase activity (ratios between firefly and renilla signals) of each vector between the vitamin D and vehicle treated (24 hrs) groups. Vh = vehicle, VD = $1\alpha,25(OH)_2D_3$.

patients, with the CsA C0 and Cmax maintained at 200–250 ng/ML and 1200–1500 ng/ML, respectively for every patient and prednisone for 16 mg PO, q.d.

MMF (Hoffman-La Roche) (1 g/dose, every 12 hrs) was administrated to all patients for one week. Plasma MPA concentrations were monitored on day 8 for 12 hrs. MMF (same dose as aforementioned) and Rocaltrol (Calcitriol, Hoffman-La Roche) (0.25 μg/dose, once daily) were co-administrated to the patients for additional one week. On day 16, plasma MPA concentrations were measured again at the same time points as in day 8 for 12 hrs. The experimental design was summarized in Fig. S3. Patients were screened by physical examination and detailed laboratory tests were conducted if necessary. Patients who had co-morbid disease or liver function that deviated from the normal range were excluded from the study. All enrolled patients did not smoke or drink alcohol, and were instructed to maintain a regular diet during the trial without any use of supplements, Chinese medicine or other treatments.

Quantification of plasma MPA was conducted by mixing patient plasma sample (20 μL) and acetonitrile (800 μl) containing internal standard (osalmid, 96 ng/ml), followed by centrifugation 12000 rpm for 10 min. The supernatant was used to detect MPA using LC-MS/MS with similar settings as mentioned above.

Pharmacokinetic analysis. Pharmacokinetic parameters were estimated using a noncompartmental analysis. The maximum serum MPA concentrations (Cmax) and time to reach Cmax (Tmax) were determined by visual inspection of the serum MPA concentration-time curves. The terminal elimination rate constant (k) was calculated by least-squares linear regression of the log-linear portion of the serum concentration-time curves. The area under the serum concentration-time curve from 0 to 12 hours ($AUC_{0\text{-}12}$) was calculated using the linear trapezoidal rule. Since MMF is rapidly and completely hydrolyzed to MPA, the oral clearance (CL/F) of MPA was estimated by the ratio of the MMF dose (corrected for differences in the molecular weight) and the AUC of the dosing interval.

Data analyses and statistics. Comparison between treatments in cell lines was conducted using an unpaired t-test. The correlation between VDR and UGT gene

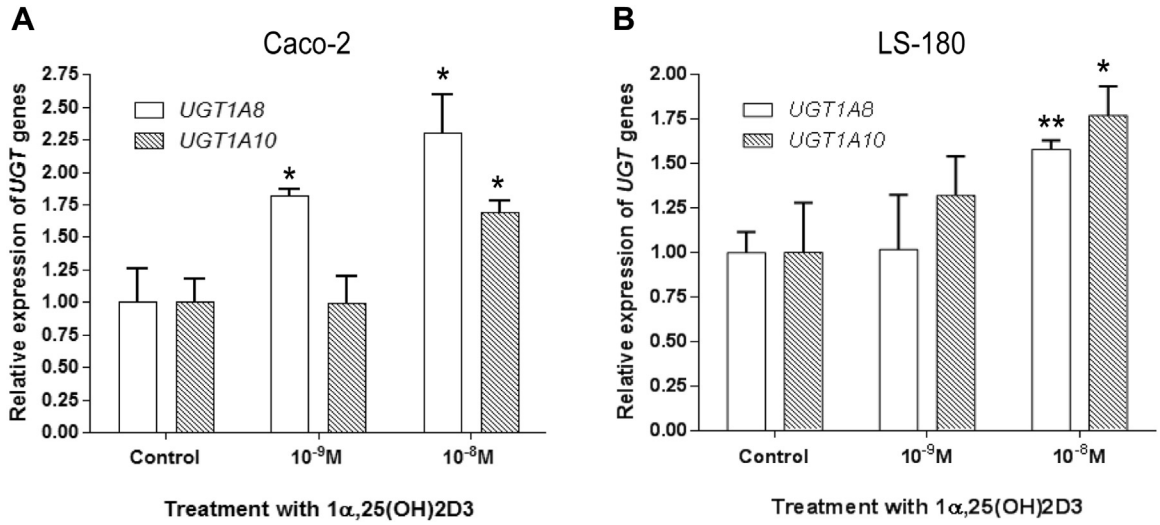

Fig 3. Induction of *UGT1A8* and *UGT1A10* by the $1\alpha,25(OH)_2D_3$ treatment in Caco-2 (**A**) and LS180 (**B**) cells. Data were shown as mean ± SD for each treatment group. The ratio of expression level between each *UGT* relative to that of the *18S* gene was normalized to that of the control group. $*P < 0.05$; $**P < 0.01$. *P* values were calculated based on the comparison between the $1\alpha,25(OH)_2D_3$ treatment group and control group. Transcription levels of both *UGT1A8* and *UGT1A10* were not detectable in HCT-116 before and after $1\alpha,25(OH)_2D_3$ treatment and therefore were not shown.

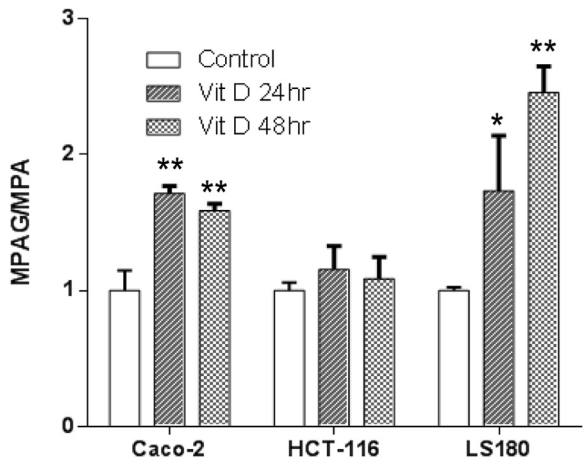

Fig 4. Induction of UGT activities for glucuronidation of MPA by $1\alpha,25(OH)_2D_3$ in Caco-2, HCT-116 and LS180 cells. The ratio between MPAG and MPA levels was normalized to that of the control group. Data were shown as mean ± SD for each treatment group. $*P < 0.05$; $**P < 0.01$. *P* values were calculated based on the comparison between the $1\alpha,25(OH)_2D_3$ treatment group and control group for each cell line.

expression was performed with linear regression. A paired t-test was used to compare the difference in PK parameters before and after vitamin D treatment in transplantation patients. The type I error rate was set to 0.05 for all comparisons. Data were analyzed and plotted using Graphpad InStat 3.0 and Prism 6.0, respectively (CA, USA).

RESULTS

Identification and confirmation of the VDREs in the UGT1A region. Our bioinformatic analysis of ~200 kb region of the entire *UGT1A* locus reveals a total of 83 putative DR3-type VDREs in the region, with 13 of which distributed within the *UGT1A8-UGT1A10* ± 10kb region (see supplemental Table SI for more details). However, the two ChIP-seq identified VDREs were not predicted in our list, suggesting that they might be motifs that are different from DR3-type.

To validate these VDR binding sites, we used three human colorectal cancer cell lines: LS180, Caco-2 and HCT-116. We first conducted ChIP assays for the two ChIP-seq identified VDREs (CS1 and CS2) as well as 4 putative VDREs (No. 16, 17, 21 and 22) closest to the *UGT1A8* or *UGT1A10* exon 1 region (Table SI). Positive binding of VDR to the locus 16 (VDRE16) (approximately 5.5kb upstream from *UGT1A8* exon 1, Chr 2: 234,520,791–234,520,805) was observed in all 3 cell lines especially at the time point of 24 hr (Fig 1A). Both ChIP-seq identified VDR binding regions showed strong VDR binding after 24 hrs of vitamin D treatment in LS180 (Fig 1B) but not in Caco-2 or HCT-116 (Fig. S2). No significant binding of VDR to the remaining 3 tested loci (17, 21 and 22) has been observed (data not shown).

Cloning and luciferase assay. To further validate the D3 regulation on *UGT1A8* and *UGT1A10* gene expression, we respectively cloned the three DNA fragments (CS1, CS2 and VDRE16) into the upstream region of

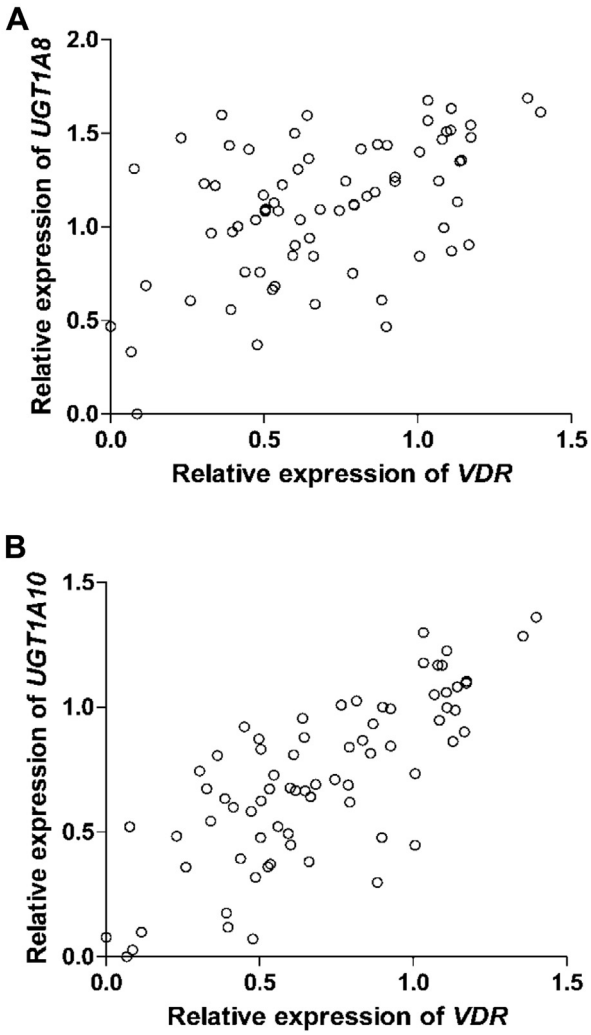

Fig. 5. Pearson correlation between the gene expression of *VDR* and *UGT1A8* (**A**) and *UGT1A10* (**B**) in human normal colorectal tissue samples. The expression of *VDR* and *UGT* genes was relative to that of the *18S* gene. The ratios were further normalized to the lowest value of the 73 samples and log transformed (+log10).

the SV40 promoter of the pGL3-promoter vector. Transient transfection of all three constructs into the LS180 demonstrated that these VDR binding sites significantly enhanced the reporter gene promoter activity under $1\alpha,25(OH)_2D_3$ treatment as compared to the pGL3-Promoter vector or the control group with vehicle only. The luciferase activity was increased about 40–60% in these cells after $1\alpha,25(OH)_2D_3$ treatment ($P < 0.05$ for all tests) (Fig 2).

Induction of UGT1A8 and UGT1A10 expression by $1\alpha,25(OH)_2D_3$ treatment. We then tested whether the transcription of both *UGT* genes was inducible by $1\alpha,25(OH)_2D_3$. After treatment of all 3 cells with $1\alpha,25(OH)_2D_3$ for 24 hrs, significantly increased expression of both *UGT1A8* and *UGT1A10* was observed in LS180 and Caco-2 but not in the HCT-116 cell line (Fig 3). The induction of both *UGT1A8* and *UGT1A10* was dose-dependent in Caco-2 and LS180, respectively, with significantly increased expression of both genes observed in both cell lines under the higher concentration (10^{-8} M) ($P < 0.05$ for all tests). Real-time PCR analysis demonstrated that both *UGT* genes were not detectable in HCT-116 cell lines with or without any treatment (data not shown).

Regulation of MPA glucuronidation activity in vitro by $1\alpha,25(OH)_2D_3$. We further examined whether MPA metabolism is altered after $1\alpha,25(OH)_2D_3$ induction for *UGT1A8* and *UGT1A10* expression. All 3 cells were treated with $1\alpha,25(OH)_2D_3$ for 24 hrs or 48 hrs and the MPA glucuronidation product MPA glucuronide (MPAG) was measured. We found that MPA glucuronidation activity in both Caco-2 and LS180 was significantly increased 1.6- and 2.5-fold after 48 hrs of induction, respectively ($P < 0.002$), but not in the HCT-116 cells ($P = 0.22$) (Fig 4), which is consistent with the induction results for the transcription of two *UGT*s by $1\alpha,25(OH)_2D_3$ among these 3 cells.

Gene expression of VDR, UGT1A8 and UGT1A10 genes in human colorectal tissue. In order to examine whether the VDR regulation for both *UGT* genes also exists *in vivo*, we quantified the mRNA levels of all three genes in a set of normal colorectal tissue samples (n = 73). We found that all three genes were highly expressed in human colorectal tissue. There was a highly significant positive correlation in the expression level between *VDR* and the *UGT1A8* (r = 0.49, $P < 0.0001$) or *UGT1A10* (r = 0.77, $P < 0.0001$) gene (Fig 5).

Impact of $1\alpha,25(OH)_2D_3$ on MMF/MPA pharmacokinetics. Based on the aforementioned mechanistic study *in vitro* or *ex vivo*, we hypothesize that $1\alpha,25(OH)_2D_3$ intake may significantly change the MMF/MPA pharmacokinetics. To test this hypothesis, we compared the PK profile of MPA before and after $1\alpha,25(OH)_2D_3$ intake in human kidney transplantation recipients (n = 10). We found that one-week of $1\alpha,25(OH)_2D_3$ treatment significantly reduced the MPA $AUC_{0\text{-}12}$ and maximum concentration (Cmax) by about 40% in these patients ($P = 0.0008$ and $P = 0.003$, respectively), while the oral clearance (CL/F) of MPA was significantly increased over 70% ($P = 0.008$) (Fig 6). No statistically significant relationships were observed between age, gender, BMI or weight with these parameters ($P > 0.05$, data not shown). Effect of other clinical factors including Cr, CrCL and Albumin levels on PK parameter changes were also tested and no statistically significant impact were observed ($P > 0.05$, data not shown).

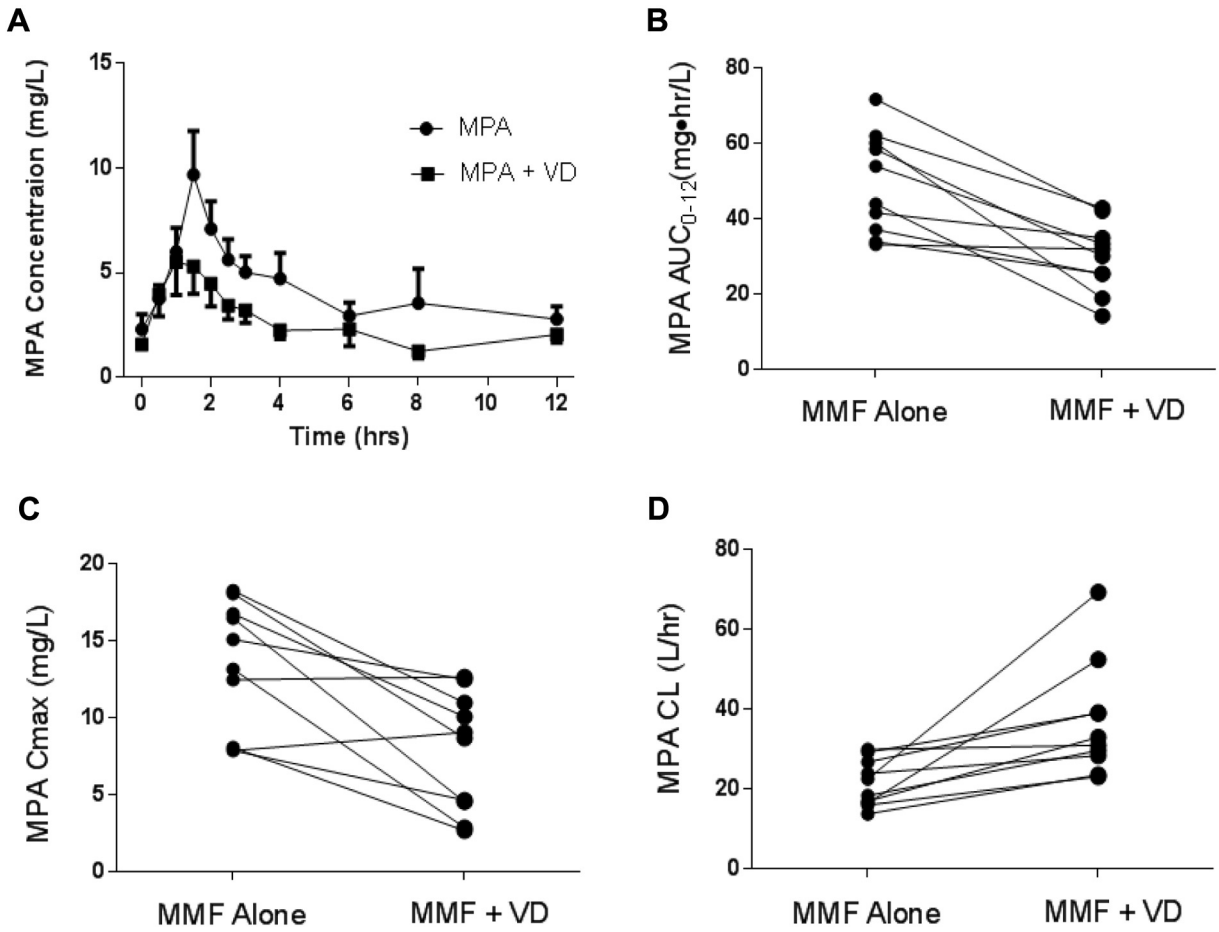

Fig. 6. Impact of $1\alpha,25(OH)_2D_3$ on MPA pharmacokinetics: **A**) MPA concentration changes in 12 hours; **B**) Paired comparison of MPA area-under-the-curve ($AUC_{0\text{-}12}$). Data for each time point was shown as mean ± SEM; **C**) Paired comparison of MPA Cmax; and **D**) Paired comparison of MPA clearance. VD = $1\alpha,25(OH)_2D_3$.

DISCUSSION

Our study for the first time demonstrates that vitamin D significantly alters the metabolism of MPA by modulating the expression of two intestinal UGTs *in vitro*. This effect may further lead to an altered MPA pharmacokinetics when MPA and vitamin D are co-administrated. This modulation may in part explain the inter- and intra-individual differences in MPA PK observed clinically. More importantly, our findings have critical clinical implications. Previous studies have indicated that the MPA PK parameters are significantly associated with various clinical outcomes in renal transplant recipients as well as adverse events.[4,6,7] This calcitriol-MPA interaction, especially during calcitriol co-administration or dietary supplementation may potentially reduce the efficacy of MMF and increase the risk of organ rejection. This is particularly an issue as osteoporosis e.g. bone loss and fracture, is a common and serious morbidity in kidney transplantation, and calcitriol is increasingly used to reduce the accelerated bone loss in renal transplant recipients.[26,27]

Understanding the inter-individual variability in the gene expression of drug metabolism enzymes in different tissues or organs is tremendously important for individualizing medication. Compared to hepatic *UGT*s, there are very limited studies on the genetic basis for the regulation of *UGT1A8* and *UGT1A10*, which are predominantly expressed in human intestinal tissue.[15,19] Our study suggests that intestinal regulation of *UGT* genes is also important in the pharmacokinetics of therapeutic agents. Although other UGTs e.g. UGT1A9 and UGT2B7 were also shown to be involved in MPA glucuronidation,[10-14] our previous study demonstrated that VDR is not a significant regulator for hepatic UGTs.[28] This suggests that this vitamin D-UGT modulation may be tissue-specific. It

is now important to consider both the hepatic and extrahepatic metabolism in order to completely understand the inter-patient variability in MPA PK and/or efficacy. In addition, given the numerous therapeutic agents that are substrates of UGT1A8 and/or UGT1A10,[18,21,29-34] we suggest that caution should be exercised when vitamin D is co-administered.

Given the large number of *in silico*-predictive putative VDREs at the *UGT1A* locus, we did not validate all of them in our study. Rather, we focused our validation on the putative VDREs closest to the *UGT1A8* and *UGT1A10* regions. Our subsequent *in vitro* and *ex vivo* assays strongly suggested that intestinal *UGT1A8* and *UGT1A10* are VD-regulated genes. This finding is consistent with the recent genome-wide ChIP-seq study by Meyer MB et al,[24] where VDR binding sites were identified in the *UGT1A* region and *UGT1A* transcription was significantly induced by vitamin D treatment in the LS180 cell. However, the VDRE16 identified in our study was not observed in this ChIP-seq assay in LS180, and our confirmatory assay also did not observe the two loci identified in their study in Caco-2 and HCT-116 cells. While this may be due to the different cell lines used which further reflects a potential cell-specific usage of the VDREs, it also suggests that additional types of VDREs are located in the region since no DR3-type of VDRE was predicted in the two loci identified by the ChIP-seq. Further analyses are now ongoing in the lab to elucidate the detailed VDR binding mechanism to these VDREs. Nevertheless, our results combined with the findings in Meyer's study provide evidence that multiple VDREs may be distributed in the entire locus. As ChIP-seq has been the unequivocal strategy in identifying transcription factor-binding DNA elements, a comprehensive ChIP-seq analysis in multiple cell lines derived from intestinal tissue under different treatment options may eventually unravel the detailed mechanism underlying the VDR regulation of the two UGTs.

We did not observe induction of either *UGT* in HCT-116 cells, although the ChIP assay demonstrated a strong VDR binding to the identified VDRE16 in this cell (Fig 2). An explanation is that additional mechanisms may be involved in the inactivation of the two UGT genes in this cancer cell line. There is no expression of the two *UGT* genes in the non-treated HCT-116 cells in our real-time PCR assay, which was in contrast to the relatively higher basal expression in the Caco-2 or LS180 cells (data not shown). Interestingly, it has been reported that DNA methylation represses *UGT1A1* expression in colon cancer cells, in particular HCT-116.[35,36] It is thus reasonable that a similar mechanism may be involved in the inactivation of *UGT1A8* and *UGT1A10* in this cell.

MPA is a widely used and important immunosuppressant medication that requires specific therapeutic levels for optimal clinical efficacy. The potential clinical implications of our findings clearly support more research to further elucidate the regulation of these two UGT enzymes by vitamin D and the VDR. This research is all the more imperative, given the ubiquitous and seemingly innocuous clinical practice of providing vitamin D supplementation to patients.

ACKNOWLEDGMENTS

This work was supported by in part by the start-up fund (W.L.) from the Department of Medicinal Chemistry and Molecular Pharmacology, Purdue University, and National Natural Science Foundation of China (Grant 81270557, 81000188).

All authors have read the journal's authorship agreement.

All authors have read the journal's policy on conflicts of interest, and all authors declared no conflicts of interest.

REFERENCES

1. Guerra G, Ciancio G, Gaynor JJ, et al. Randomized trial of immunosuppressive regimens in renal transplantation. J Am Soc Nephrol 2011;22:1758–68.
2. Ekberg H, Bernasconi C, Tedesco-Silva H, et al. Calcineurin inhibitor minimization in the Symphony study: observational results 3 years after transplantation. Am J Transplant 2009;9:1876–85.
3. Ekberg H, Tedesco-Silva H, Demirbas A, et al., Study, EL-S. Reduced exposure to calcineurin inhibitors in renal transplantation. N Engl J Med 2007;357:2562–75.
4. Gellermann J, Weber L, Pape L, Tonshoff B, Hoyer P, Querfeld U, Gesellschaft fur Padiatrische, N. Mycophenolate mofetil versus cyclosporin A in children with frequently relapsing nephrotic syndrome. J Am Soc Nephrol 2013;24:1689–97.
5. Staatz CE, Tett SE. Pharmacology and toxicology of mycophenolate in organ transplant recipients: an update. Arch Toxicol 2014;88:1351–89.
6. van Hest RM, Mathot RA, Pescovitz MD, Gordon R, Mamelok RD, van Gelder T. Explaining variability in mycophenolic acid exposure to optimize mycophenolate mofetil dosing: a population pharmacokinetic meta-analysis of mycophenolic acid in renal transplant recipients. J Am Soc Nephrol 2006;17:871–80.
7. Knight SR, Morris PJ. Does the evidence support the use of mycophenolate mofetil therapeutic drug monitoring in clinical practice? A systematic review. Transplantation 2008;85:1675–85.
8. Mathew TH. A blinded, long-term, randomized multicenter study of mycophenolate mofetil in cadaveric renal transplantation: results at three years. Tricontinental Mycophenolate Mofetil Renal Transplantation Study Group. Transplantation 1998;65:1450–4.
9. Chen H, Chen B. Clinical mycophenolic acid monitoring in liver transplant recipients. World J Gastroenterol 2014;20:10715–28.
10. Bernard O, Tojcic J, Journault K, Perusse L, Guillemette C. Influence of nonsynonymous polymorphisms of UGT1A8 and UGT2B7 metabolizing enzymes on the formation of phenolic and acyl glucuronides of mycophenolic acid. Drug Metab Dispos 2006;34:1539–45.

11. Joy MS, Boyette T, Hu Y, et al. Effects of uridine diphosphate glucuronosyltransferase 2B7 and 1A7 pharmacogenomics and patient clinical parameters on steady-state mycophenolic acid pharmacokinetics in glomerulonephritis. Eur J Clin Pharmacol 2010;66:1119–30.
12. van Schaik RH, van Agteren M, de Fijter JW, et al. UGT1A9 -275T>A/-2152C>T polymorphisms correlate with low MPA exposure and acute rejection in MMF/tacrolimus-treated kidney transplant patients. Clin Pharmacol Ther 2009;86:319–27.
13. Levesque E, Delage R, Benoit-Biancamano MO, et al. The impact of UGT1A8, UGT1A9, and UGT2B7 genetic polymorphisms on the pharmacokinetic profile of mycophenolic acid after a single oral dose in healthy volunteers. Clin Pharmacol Ther 2007;81: 392–400.
14. Mackenzie PI. Identification of uridine diphosphate glucuronosyltransferases involved in the metabolism and clearance of mycophenolic acid. Ther Drug Monit 2000;22:10–3.
15. Tukey RH, Strassburg CP. Human UDP-glucuronosyltransferases: metabolism, expression, and disease. Annu Rev Pharmacol Toxicol 2000;40:581–616.
16. Guillemette C, Levesque E, Harvey M, Bellemare J, Menard V. UGT genomic diversity: beyond gene duplication. Drug Metab Rev 2010;42:24–44.
17. Mackenzie PI, Bock KW, Burchell B, et al. Nomenclature update for the mammalian UDP glycosyltransferase (UGT) gene superfamily. Pharmacogenet Genomics 2005;15:677–85.
18. Gregory PA, Lewinsky RH, Gardner-Stephen DA, Mackenzie PI. Regulation of UDP glucuronosyltransferases in the gastrointestinal tract. Toxicol Appl Pharmacol 2004;199:354–63.
19. Zhang W, Liu W, Innocenti F, Ratain MJ. Searching for tissue-specific expression pattern-linked nucleotides of UGT1A isoforms. PLoS One 2007;2:e396.
20. Mizuma T. Impact of intestinal metabolism on drug development. Nihon Yakurigaku Zasshi 2009;134:142–5.
21. Mizuma T. Intestinal glucuronidation metabolism may have a greater impact on oral bioavailability than hepatic glucuronidation metabolism in humans: a study with raloxifene, substrate for UGT1A1, 1A8, 1A9, and 1A10. Int J Pharm 2009;378:140–1.
22. Pike JW. Genome-wide principles of gene regulation by the vitamin D receptor and its activating ligand. Mol Cell Endocrinol 2011;347:3–10.
23. Fleet JC, Schoch RD. Molecular mechanisms for regulation of intestinal calcium absorption by vitamin D and other factors. Crit Rev Clin Lab Sci 2010;47:181–95.
24. Meyer MB, Goetsch PD, Pike JW. VDR/RXR and TCF4/beta-catenin cistromes in colonic cells of colorectal tumor origin: impact on c-FOS and c-MYC gene expression. Mol Endocrinol 2012;26:37–51.
25. Toell A, Polly P, Carlberg C. All natural DR3-type vitamin D response elements show a similar functionality in vitro. Biochem J 2000;352:301–9.
26. Dounousi E, Leivaditis K, Eleftheriadis T, Liakopoulos V. Osteoporosis after renal transplantation. Int Urol Nephrol 2015;47: 503–11.
27. Jeon HJ, Han M, Jeong JC, et al. Impact of vitamin D, bisphosphonate, and combination therapy on bone mineral density in kidney transplant patients. Transplant Proc 2013;45:2963–7.
28. Liu W, Ramirez J, Gamazon ER, et al. Genetic factors affecting gene transcription and catalytic activity of UDP-glucuronosyltransferases in human liver. Hum Mol Genet 2014;23:5558–69.
29. Cheng Z, Radominska-Pandya A, Tephly TR. Studies on the substrate specificity of human intestinal UDP- lucuronosyltransferases 1A8 and 1A10. Drug Metab Dispos 1999;27:1165–70.
30. Dellinger RW, Chen G, Blevins-Primeau AS, Krzeminski J, Amin S, Lazarus P. Glucuronidation of PhIP and N-OH-PhIP by UDP-glucuronosyltransferase 1A10. Carcinogenesis 2007;28: 2412–8.
31. Itaaho K, Court MH, Uutela P, Kostiainen R, Radominska-Pandya A, Finel M. Dopamine is a low-affinity and high-specificity substrate for the human UDP-glucuronosyltransferase 1A10. Drug Metab Dispos 2009;37:768–75.
32. Argikar UA, Remmel RP. Effect of aging on glucuronidation of valproic acid in human liver microsomes and the role of UDP-glucuronosyltransferase UGT1A4, UGT1A8, and UGT1A10. Drug Metab Dispos 2009;37:229–36.
33. Balliet RM, Chen G, Gallagher CJ, Dellinger RW, Sun D, Lazarus P. Characterization of UGTs active against SAHA and association between SAHA glucuronidation activity phenotype with UGT genotype. Cancer Res 2009;69:2981–9.
34. Miksits M, Maier-Salamon A, Vo TP, et al. Glucuronidation of piceatannol by human liver microsomes: major role of UGT1A1, UGT1A8 and UGT1A10. J Pharm Pharmacol 2010;62:47–54.
35. Gagnon JF, Bernard O, Villeneuve L, Tetu B, Guillemette C. Irinotecan inactivation is modulated by epigenetic silencing of UGT1A1 in colon cancer. Clin Cancer Res 2006;12:1850–8.
36. Belanger AS, Tojcic J, Harvey M, Guillemette C. Regulation of UGT1A1 and HNF1 transcription factor gene expression by DNA methylation in colon cancer cells. BMC Mol Biol 2010;11:9.

APPENDIX

METHODS

Bioinformatic analysis. The entire *UGT1A* locus and ±100kb flanking region (a total of 352,020 bp) were screened for putative VDREs. Although there are different types of VDREs, we only focused on the most typical DR3 type consensus sequence, i.e. the direct repeat (DR) of the hexameric core sequence RGDKYR (R = G or A, D = A, G or T, K = G or T, Y = C or T).[1] The online "DNA Pattern Find" program (http://www.ualberta.ca/~stothard/javascript/dna_pattern.html) was used for the motif screening.

Cell culture and treatment with 1α,25(OH)$_2$D$_3$. Caco-2, HCT-116 and LS180 cell lines were obtained from American Type Culture Collection (Manassas, VA, USA) and maintained in Dulbecco's modified Eagle's medium containing 10% fetal bovine serum, 50 μg/ml penicillin, 0.25 μg/ml streptomycin, and 2 mM L-glutamine at 37°C with 5% CO_2.Cells were treated with 1α,25(OH)$_2$D$_3$ (Sigma, MO, USA) at 10^{-9} M and 10^{-8} M for 1, 8, 24 or 48 hrs for different tests.

Effects of 1α,25(OH)$_2$D$_3$ treatment on MPA glucuronidation in cell lines. MPA glucuronidation was quantified using HPLC/MS. Briefly, the sample preparation followed that of Klepacki, et al.[2] In short, protein precipitation was performed using a solution of 30% 0.2 M ZnSO4 in water and 70% methanol. Separation was performed on an Agilent Rapid Res 1200 HPLC system using an Agilent Zorbax XDB-C8 (2.1 × 50 mm, 3.5 μm) column. Mobile phase A was water with 0.1% formic acid and 2 mM NH4Ac. Mobile phase B was 5% water and 95% methanol, with 0.1% formic acid and 2 mM NH4Ac. Gradient elution was used, increasing mobile phase B from 30% to 100% in 10 min. The column was re-equilibrated at 30% B for 5 minutes prior to subsequent injection. A flow rate of 0.3 mL/min was used. Retention time for MPA was 8.8 minutes and for MPAG was 6.7 minutes.

Analytes were quantified by MS/MS utilizing an Agilent 6460 triple quadrupole mass spectrometer with positive electrospray ionization (ESI). A fragmentor energy of 125 V and a dwell time of 150 ms was used. Source parameters were as follows: nitrogen gas temp = 325°C and flow rate = 9 L/min, nebulizer pressure = 35 psi, sheath gas temperature = 275°C, sheath gas flow rate = 7 L/min, and capillary potential = 3.0 kV. Quantitation was based on Multiple Reaction Monitoring (MRM). Maximum sensitivity was obtained by monitoring the corresponding sodium and ammonium adducts, as the protonated adduct response was negligible.[3] Respective adduct responses were summed for calculations. For MPA, [MPA + Na]+ m/z 343.0 to 229.1 and [MPA + NH4]+ m/z 338.0 to 207.0. For MPAG, [MPAG + Na]+ m/z 519.0 to 229.1 and [MPAG + NH4]+ m/z 514.0 to 207.0. All transitions used a collision energy of 15 eV and a dwell time of 150 ms. All data were collected and analyzed with Agilent Mass Hunter B.03 software. To calculate the MPA-MPAG turnover rate, MPA and MPAG peak areas were quantified. The detection limits (peak area) for MPA and MPAG are 600 and 45, while the MPA and MPAG peak areas in the samples ranged 1 million to 4 million and 2000–50000, respectively. Therefore the peak areas were all well above the detection limits.

Chromatin Immunoprecipitation (ChIP) assay. Caco-2, HCT-116 and LS180 cells were treated with 10^{-8} M 1α,25(OH)$_2$D$_3$ or vehicle (ethanol) for 1, 8 and 24 hours, respectively. The cells were cross-linked by adding 270 μL formaldehyde to 10 mL medium for 10 min, and the reaction was stopped by 0.125 M glycine (final concentration). Cell lysates were sonicated to generate 200–1,000 bp DNA fragments. Antibodies against VDR (Millipore-Chemicon, MO, USA) were used to immunoprecipitate the DNA-protein complexes. Normal IgG was used as a negative control. After an overnight incubation with the antibody, the immune complexes were collected using 80 μL of protein A Agarose slurry (Upstate Biotechnology, CA, USA). The beads were washed twice with the following buffers (Upstate Biotechnology, CA, USA): low salt washing buffer, high salt wash buffering, LiCl washing buffer, and TE buffer. The DNA was eluted with 1% SDS and 0.1 M $NaHCO_3$ elution buffer, and then subjected to reverse cross-linking, proteinase digestion, and purification using a commercial kit (Qiagen, Valencia, CA). Among the 83 candidate VDREs, 4 (No. 16, 17, 21, and 22 see Table SI) were tested for VDR binding. We hypothesized that these 4 loci are the closest to *UGT1A8* and *UGT1A10* exon 1s, which may possess strongest regulation for these two *UGT* genes. The primers used to amplify the 4 candidate VDRE regions were 1A8VDRr16-F: 5′-CAGGTATACACGTGCCATGGT-3′, 1A8VDRr16-R: 5′-CCGCATGCTCTCACACATAAG-3′; 1A8VDRr17-F: 5′-CCATCTGCAAGTAATTCCCTTC-3′, 1A8VDRr17-R: 5′-CACCAGGTGTTTCATCTGGATT-3′; 1A10VDRr21-F: 5′-CTGCAGTCATGGCATAGCTTT-3′, 1A10VDRr21-R: 5′-GTGTGGATCCACTTATATGCAG-3′; and 1A10VDRr22-F: 5′-CCATCTGCAAGTAATTCCCTTG-3′, 1A22VDRr10-R: 5′-ACACCAGGTGTTTCATCTGGAT-3′. The two VDR binding sites (CS1 and CS2) identified in the recently published ChIP-seq study in LS180 cell[4] were also tested in our samples. These two loci were

located at chr2:234,668,582–234,669,759 and chr2:234,672,790–234,673,397 (hg19). The primers used to amplify these two loci were CS1-1F:

CS1-1F: 5′-CTCCCTGCTACCTTTGTGGACT-3′
CS1-1R: 5′-CGTCAGGTGCTAGGACAACTAT-3′
CS1-2F: 5′-GTCATGCTGACGGACCCTT-3′
CS1-2R: 5′-GGGCCTAGGGTAATCCTTCA-3′
CS2-1F: 5′-GCTGGCTCAGGTAGGAGTTG-3′ and
CS2-1R: 5′-CCACTCAGCAATCAGCAGGA-3′, respectively. PCR amplification was cycled 35 times at 95°C for 10s, 56°C for 20s and 72°C for 30s after preheating at 95°C for 10 min. The PCR products were separated and visualized by electrophoresis with 2% Agarose gel. ChIP assays were repeated three times and the representative data are shown. A typical electrophoretic separation of the ChIP-PCR products in agrose gel was shown in Fig. S1.

Cloning and luciferase assay. The DNA fragment of 185 bp, 330 bp and 178 bp containing VDRE16,CS1-1 and CS2 were generated with PCR and cloned into the pGL-3-Promoter (pGL3-P) vector containing the *firefly* luciferase gene (Promega, WI, USA). For the CS1 site, we only cloned the CS1-1 fragment as this site was demonstrated to have the strongest VDR binding in the ChIP assay (Fig 1). Cloned sequences were verified by sequencing. For luciferase assay, the pRL-TK plasmids containing a *renilla* luciferase gene (Promega) was co-transfected with pGL3-P or pGL3-P-VDRE vectors into LS180 cells, using Lipofectamine 2000 Reagent (Invitrogen, CA, USA) according to manufacturer's instruction. Cells were treated with vehicle (ethanol) or 10^{-8} M $1\alpha,25(OH)_2D_3$ for 24 hs after the transfection. Cells were then harvested and the *firefly* and *renilla* luciferase activities were then measured by using the Dual-Light Luciferase Assay Kit (Promega) according to the manufacturer's instructions. The *firefly* luciferase activity was normalized to that of the *renilla* to obtain the relative activity. For plotting the data, all measurements were also normalized to the relative activity value of the pGL3-Ptransfection treated with vehicle only. Experiments were repeated twice and the representative data are shown.

DNA and RNA extraction and reverse transcription. The total RNA of the cells as well as both the RNA and DNA of the human colorectal tissue samples were extracted by using the RNA/DNA Mini Kit (Qiagen, Hilden, Germany). The integrity of the cell and tissue RNA was checked by separated in 1% Agarose gel (Fig. S1), and concentration was measured by ultraviolet spectroscopy. Complementary DNA (cDNA) was made by reverse transcription of total RNA (1 μg) by using the High-Capacity cDNA Archive Kit (Applied Biosystems, CA, USA).

Real-time PCR. Gene expression levels of *UGT1A8*, *UGT1A10* and/or *VDR* were quantified with real-time PCR by using the SYBR Green Super Mix (Bio-Rad, CA, USA) in the Eppendorf Realplex real-time PCR system (Eppendorf, Germany) according to the protocol previously established in the lab.[5,6] Briefly, amplicons in *UGT1A8* and *UGT1A10* (161 bp and 187 bp, respectively), amplified with primers spanning exon 1 and 2, and *VDR* (107 bp), sequence spanning exons 6–7, were generated by real-time PCR. The ribosomal *18S rRNA* gene and beta-actin gene (*ACTB*) were used as internal controls.[5,6] Primer sequences used for the three genes were UGT1A8F: 5′-CACATCAATTTGG TTGTTGCGACCA-3′; UGT1A8R: 5′-CCACAATTC CATGTTCTCCAG-3′; UGT1A10 F: 5′-GTCACGGC ATATGATCTCTACGGT-3′, UGT1A10 R: 5′-CCAC AATTCCATGTTCTCCAG-3′; and VDRF: 5′-TCCTC CTGCTCAGATCACTG-3′, VDRR: 5′-AGGGTCACA GAAGGGTCATC-3′. Reactions were performed with standard curves for each gene and repeated twice. Real-time PCR was cycled 45 times at 95°C for 30s, 63°C (*UGT1A8* and *UGT1A10*) or 55°C (*VDR*,*18S and ACTB*) for 1 min and 72°C for 30s after preheating at 95°C for 10 min. The relative expression levels of *UGT1A8*, *UGT1A10* and *VDR* were normalized by that of *18S*or *ACTB*, respectively. For each gene, the ratio of its expression relative to *18S*or *ACTB* was then normalized to that of the sample with the lowest gene expression level.

Real-time PCR for *UGT1A8* and *UGT1A10* in the induction assay was performed using the same conditions mentioned above. The ratio of *UGT* gene expression relative to *18S* was normalized to that of the cells treated with vehicle only.

Pharmacokinetic analysis in kidney transplantation recipients. Patient information was summarized in Table SII. The experimental design for the clinical investigation was shown in Fig S3.

Statistical analyses. Gene expression (relative ratio between each target gene and *18S rRNA* or *ACTB* gene) was log transformed (+log10) prior to the correlation analysis. Comparison of the induction of *UGT* gene expression as well as luciferase activity between the cells treated with different concentration of $1\alpha,25(OH)_2D_3$ and vehicle only were performed with non-paired t-test. Inter-individual variability in the expression of *UGT1A8* and *UGT1A10* gene was defined by using the median and distribution range. Correlations between the *VDR* gene and each *UGT* gene were performed using Pearson correlation. $P = 0.05$ was set as the cut-off for statistical significance. All statistical analysis was performed and plotted using GraphPad Prism

version 6.0 for Windows (GraphPad Software, San Diego, CA, USA).

RESULTS

ChIP assay. No significant binding of VDR to the two loci (CS1 and CS2) identified by the previous ChIP-seq study[4] was observed in Caco-2 or HCT-116. Results of the ChIP assays for these loci are shown in Fig. S2.

Candidate VDREs identified from the UGT1A8-UGT1A10 region. Table SI listed all identified candidate VDERs in the *UGT1A* locus. These are putative DR3-type VDREs in the *UGT1A*±100kb region. The core motifs are highlighted in bold. The position of start and end nucleotides of the core motifs on chromosome 2 were based on the human genome assembly hg19 (2009). The four putative VDREs (16, 17, 21 and 22) tested for VDR binding using ChIP assay were highlighted in red. Note that the exon 1 of *UGT1A8* and *UGT1A10* is between 16 and 17, and 21 and 22, respectively.

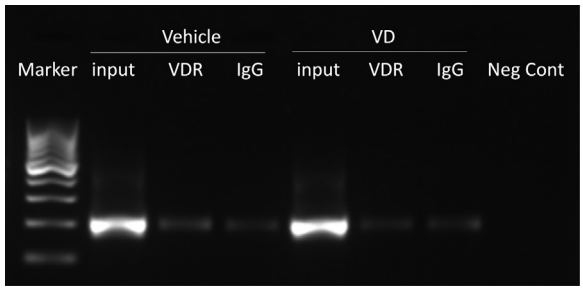

Fig S1. A typical semi-quantitative ChIP assay separated in agrose gel. Showing here is the ChIP-PCR reaction in LS180 cells for VDRE16 element under 1h vit D treatment.

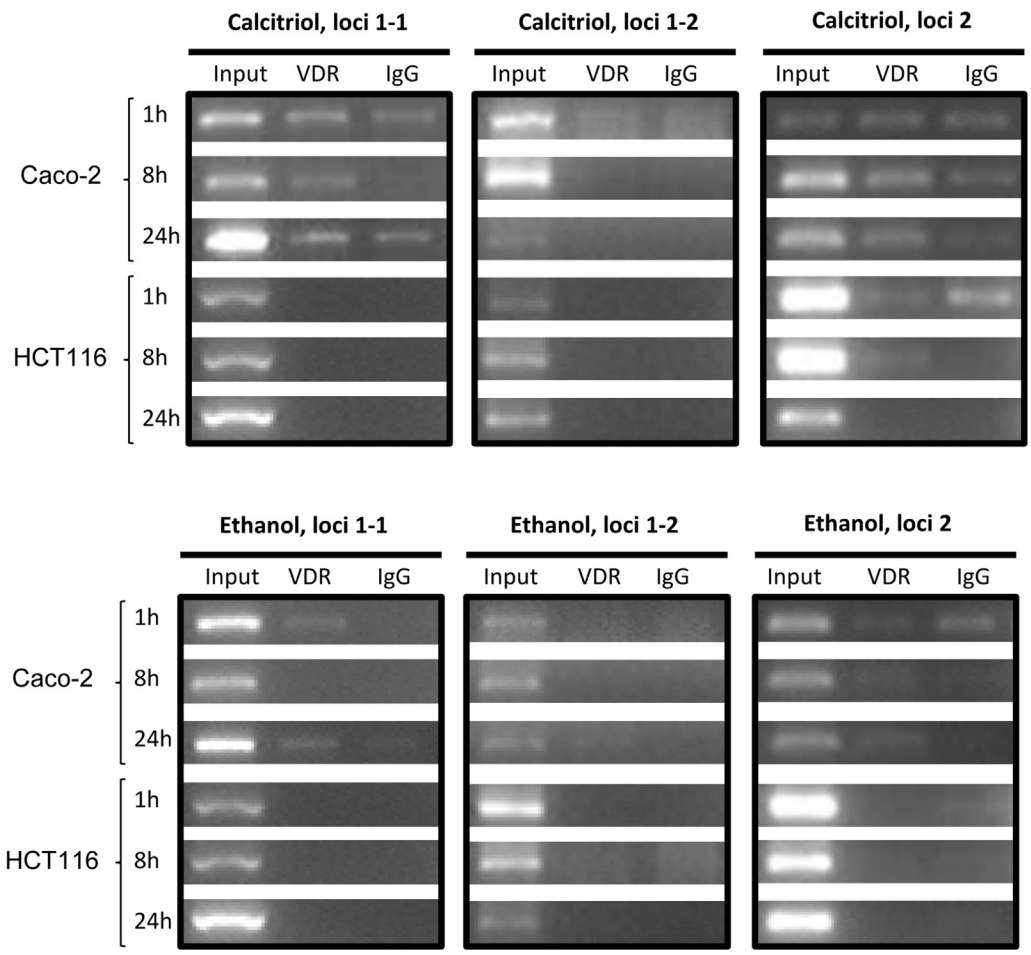

Fig S2. ChIP assay for CS1 and CS2 in Caco-2 and HCT-116 cells.

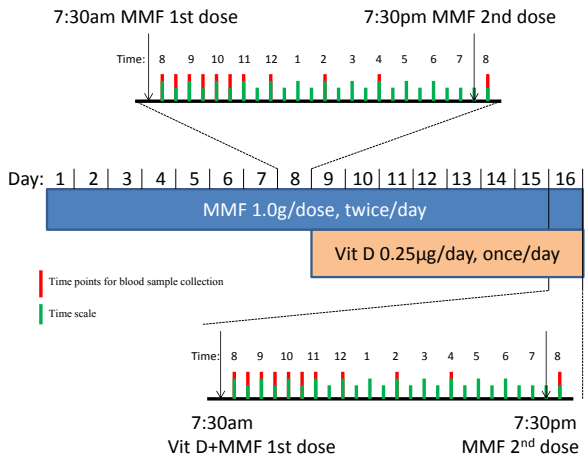

Fig S3. Experimental design for the pharmacokinetic study of MPA.

Table SI. Putative VDREs identified in the *UGT1A* locus

Putative VDRE	Locus ID	Start	End	Strand
AGTGTGTCAGGGTTG	1	234427278	234427292	Reverse
AGATTGGTTAGGTTA	2	234439010	234439024	Reverse
AGATTATATGGAGCA	3	234444375	234444389	Forward
GGTTTATCAAGTTTA	4	234447063	234447077	Reverse
GGGGTGGAGAGGTCG	5	234469459	234469473	Forward
AGGGCAGTTAGTGTA	6	234474507	234474521	Forward
AGTGTACAGGGTTTG	7	234474516	234474530	Forward
AGGGTGTCAAGTTTG	8	234489577	234489591	Forward
AGGTCAGTGGGTGCG	9	234492359	234492373	Reverse
GGTTCAGAAAGTTTG	10	234503975	234503989	Forward
GGTTCAGAAAGTTTG	11	234505369	234505383	Forward
AGTTTGCAGAGATCA	12	234505807	234505821	Forward
GGTTTGAAGAGTTTA	13	234515068	234515082	Reverse
GGTTCATTCAGGGTA	14	234516819	234516833	Forward
GGTTTGTTGAGATCA	15	234519930	234519944	Reverse
AGGTTGATGGGTGTA	16	234520791	234520805	Reverse
AGAGTAGCCAGTTTA	17	234528550	234528564	Forward
AGGGTGTAGGGTGCA	18	234529015	234529029	Reverse
AGGGTGTCAAGATCA	19	234532422	234532436	Forward
GGTGCACTTGGTGTA	20	234534743	234534757	Forward
AGTTTATGTGGTTTA	21	234536946	234536960	Forward
AGAGTAGCCAGTTTA	22	234547178	234547192	Forward
GGTGCAGGAAGATTA	23	234549637	234549651	Reverse
GGAGTAGAAAGTTTA	24	234550733	234550747	Reverse
AGGGTAACTGGTGTG	25	234555186	234555200	Reverse
GGTTTGCCCAGATTA	26	234563963	234563977	Forward
AGAGTAGCCAGTTTA	27	234582594	234582608	Forward
AGGTTGTGGGGTGCA	28	234583091	234583105	Reverse
AGTTTGACAAGTGTG	29	234584706	234584720	Forward
AGTGTGTCAAGATCA	30	234584715	234584729	Forward
GGTGCACTTGGTGTA	31	234587120	234587134	Forward
AGATCATAAAGAGTG	32	234593405	234593419	Forward
AGGTTGGTGGGTTTA	33	234602510	234602524	Forward
AGTTTATTGAGAGTG	34	234605455	234605469	Forward
AGGGTGGGGAGATTA	35	234614156	234614170	Forward
AGGGCAGCTGGATTG	36	234614896	234614910	Forward
AGGGCACGAGGGGTA	37	234619441	234619455	Reverse
AGATTGGATGGATCA	38	234622847	234622861	Reverse
AGATCACTCAGGTCA	39	234625405	234625419	Forward
GGGTTAAATGGATTA	40	234632436	234632450	Reverse
GGGGTAGGGGGAGCG	41	234642603	234642617	Forward
AGAGCATCTGGAGTG	42	234645457	234645471	Reverse
GGATTATGGGGATTA	43	234646664	234646678	Reverse
AGGGTGGTGGGAGTG	44	234652957	234652971	Forward
AGATTAATTGGATTG	45	234655396	234655410	Forward
GGAGCAGAAAGAGCA	46	234656533	234656547	Reverse
GGATTATGGGGATTA	47	234658300	234658314	Reverse
AGGGTGGTGGGAGTG	48	234664308	234664322	Forward
GGTTCATAAAGGGTA	49	234665499	234665513	Forward
AGGGTATTAGGTGTA	50	234665508	234665522	Forward
GGAGCACACAGAGTA	51	234670019	234670033	Reverse
AGGTCAATAGGTGCA	52	234674286	234674300	Forward
AGAGTGGGAGGATCA	53	234676370	234676384	Reverse
GGGGCAAAAAGAGCA	54	234676474	234676488	Reverse
GGGTCAGGGGGTTCG	55	234682594	234682608	Forward
GGGTCGTTGGGGTCA	56	234687923	234687937	Forward
GGTGCAGTAAGAGTG	57	234695888	234695902	Forward
GGTGCACTCAGGGTG	58	234700576	234700590	Forward
AGGGCAGCAGGGTTG	59	234701359	234701373	Forward

(*Continued*)

Table SI. (*Continued*)

Putative VDRE	Locus ID	Start	End	Strand
AGTTTGTTAGGGTTG	60	234703413	234703427	Forward
AGGGTGGGTGGGGTG	61	234704971	234704985	Forward
GGGGTAGGCAGGGTG	62	234704998	234705012	Forward
GGTGTGGGGAGGGTA	63	234705145	234705159	Reverse
GGATTGTTGAGTGCA	64	234705929	234705943	Reverse
AGTGTATTAAGTGTA	65	234706167	234706181	Forward
AGATTGCACAGGTTG	66	234709678	234709692	Reverse
GGTTTGATGAGTGTG	67	234710522	234710536	Forward
AGAGTGAGAGGGGCA	68	234711578	234711592	Reverse
AGGGCAGAGGGAGTG	69	234718204	234718218	Reverse
AGATTAACAGGTTCA	70	234722047	234722061	Forward
AGATTAGGCAGTGCA	71	234723774	234723788	Forward
AGGGTGGTGAGTTTG	72	234730061	234730075	Reverse
AGGGCGGTGGGTGCA	73	234731212	234731226	Forward
GGTGTGGGCGGGGTG	74	234732328	234732342	Forward
GGGTCGATAGGTGCA	75	234736286	234736300	Forward
GGGGTGGTGAGTGCA	76	234739372	234739386	Reverse
AGTGCAACCAGGGCA	77	234741413	234741427	Forward
GGAGTGTGGGGAGCA	78	234746490	234746504	Reverse
GGGTCAGTGGGAGTG	79	234748628	234748642	Reverse
AGGGCGGCAGGAGCA	80	234759576	234759590	Forward
AGTGTGAATGGAGTA	81	234762437	234762451	Reverse
AGTGTACATAGGTTA	82	234774476	234774490	Reverse
GGGGTGGCTGGTTCA	83	234775336	234775350	Forward

Table SII. Demographic (age, gender) and clinical (BMI, blood levels of Creatinine (Cr), Albumin and clearance of Creatinine (CrCL)) information for the kidney transplantation recipients (n = 10)

Patient ID	Gender	Age	BMI	Cr (μmol/L)	CrCL (mL/min)	Albumin (g/L)
1	F	57	22.9	96	76	41.1
2	M	40	19.4	88	68	39.6
3	M	30	21.6	105	86	40.9
4	M	53	22.8	109	84	42
5	M	40	20.5	98	75	44.8
6	M	38	22.1	93	72	40.4
7	M	50	23.5	104	85	40.2
8	M	43	20.2	102	82	43.4
9	F	32	25.4	102	78	43.9
10	M	42	20.1	102	70	39.3

REFERENCES

1. Toell A, Polly P, Carlberg C. All natural DR3-type vitamin D response elements show a similar functionality in vitro. Biochem J 2000;352:301–9.
2. Klepacki J, Klawitter J, Bendrick-Peart J, et al. A high-throughput U-HPLC-MS/MS assay for the quantification of mycophenolic acid and its major metabolites mycophenolic acid glucuronide and mycophenolic acid acyl-glucuronide in human plasma and urine. J Chromatogr B Analyt Technol Biomed Life Sci 2012; 883-884:113–9.
3. Kuhn J, Gotting C, Kleesiek K. Sample cleanup-free determination of mycophenolic acid and its glucuronide in serum and plasma using the novel technology of ultra-performance liquid chromatography-electrospray ionization tandem mass spectrometry. Talanta 2010;80:1894–8.
4. Meyer MB, Goetsch PD, Pike JW. VDR/RXR and TCF4/beta-catenin cistromes in colonic cells of colorectal tumor origin: impact on c-FOS and c-MYC gene expression. Mol Endocrinol 2012;26: 37–51.
5. Ramirez J, Liu W, Mirkov S, et al. Lack of association between common polymorphisms in UGT1A9 and gene expression and activity. Drug Metab Dispos 2007;35:2149–53.
6. Liu W, Wu X, Zhang W, et al. Relationship of EGFR mutations, expression, amplification, and polymorphisms to epidermal growth factor receptor inhibitors in the NCI60 cell lines. Clin Cancer Res 2007;13:6788–95.